



# Point contact tunneling spectroscopy of the density of states in Tb–Mg–Zn quasicrystals

R. Escudero, F. Morales\*

Instituto de Investigaciones en Materiales, Universidad Nacional Autónoma de México, Apartado Postal 70-360, México, D. F. 04510, México



## ARTICLE INFO

### Article history:

Received 9 December 2015

Received in revised form 22 February 2016

Accepted 23 February 2016

Available online 02 March 2016

### Keywords:

Quasicrystals

Electronic density of states

Pseudogap

Point Contact Spectroscopy

Tunnel spectroscopy

## ABSTRACT

According to theoretical predictions the quasicrystalline (QC) electronic density of states (DOS) must have a rich and fine spiky structure which actually has resulted elusive. The problem with its absence may be related to poor structural characteristics of the studied specimens, and/or to the non-existence of this spike characteristic. Recent calculations have shown that the fine structure indeed exists, but only for two dimensional approximants phases. The aim of the present study is to show our recent experimental studies with point contact tunnel junction spectroscopy performed in samples of very high quality. The studies were performed in icosahedral QC alloys with composition  $\text{Tb}_9\text{Mg}_{35}\text{Zn}_{56}$ . We found the presence of a pseudogap feature at the Fermi level, small as compared to the pseudogap of other icosahedral materials. This study made in different spots on the QC shows quite different spectroscopic features, where the observed DOS was a fine non-spiky structure, distinct to theoretical predictions. In some regions of the specimens the spectroscopic features could be related to Kondo characteristics due to Tb magnetic atoms acting as impurities. Additionally, we observed that the spectroscopic features vanished under magnetic field.

© 2016 Elsevier B.V. All rights reserved.

## 1. Introduction

High purity single grain QC specimens obtained in different laboratories [1–4] have shown many of the intrinsic electronic properties related to electronic transport, thermal, and pseudogap characteristics [5–10]. Some examples of single grain QCs presenting macroscopically pentagonal faceting, or perfect bulk icosahedral aspect have been obtained by Fisher et al. [1,2]. Electronic transport properties studied in QCs show quite different behavior in comparison to the crystalline counterpart. For instance, the electrical resistivity as a function of temperature  $\rho(T)$  behaves differently to the crystalline metallic alloys with opposite behavior to the Matthiessen's rule; i.e., the electrical resistivity measured from high to low temperature dramatically increases [7,11–14]. One of many different physical properties of quasicrystalline alloys and approximants, is that the electronic states have the tendency to be localized at both sides of the Fermi energy, which is a different aspect to the characteristics observed in crystalline intermetallic alloys. The tendency to localization has been related to the manifestation of the metallic-insulating transition and the manifestation of weak electronic localization. In crystalline intermetallic alloys, the electronic states are extended at both sides of the Fermi energy. Experimental measurements performed on pure and single domain QC structures, show that the ratio between electrical resistances from low to high temperature increases with purity and perfection of the QC [1–4,7]. Additionally,

related to the pseudogap feature, it is important to mention that this characteristic at the Fermi level exists for both crystalline and quasicrystalline alloys, involving a Hume-Rothery stabilization mechanism, it is one of the reasons of the high thermodynamic stability for icosahedral QCs and also in crystalline intermetallic alloys. The only difference is that the pseudogap feature is deeper in QCs than in crystalline alloys [7,15,16].

The existence of the pseudogap has been probed and also the size and shape were determined with great detail using different spectroscopic techniques; tunneling, point contacts, and photoemission [17–20]. Scanning tunneling spectroscopy measurements taken on Al based QC have shown spiky local density of states (LDOS) when the spectroscopy is carried out at the nanometer scale. In observations at larger surface scale LDOS obviously is averaged and the spiky structure is smeared; the density of states resembles the total DOS [9,10]. It is important to mention that until today the most notable prediction of the fine spiky structure has been elusive and no experimental probes have detected it. Accordingly, the general consensus related to this absence of fine structure is that the initial theoretical calculations missed relevant information and the resulting spiky structure was only an artifact of the calculations [16]. The other relevant aspect could be related to the poor QC characteristics of the studied sample [18]. However, until today different arguments have been under different contexts [19,21,22].

Theoretical studies pointed out that the spiky structure on DOS is a characteristic of only small approximants in a two dimensional Penrose tiling and no related to the QC phase. Theoretical studies by Zijlstra and

\* Corresponding author.

E-mail addresses: [escu@unam.mx](mailto:escu@unam.mx) (R. Escudero), [fmleal@unam.mx](mailto:fmleal@unam.mx) (F. Morales).

Janssen, and Zijlstra and Bose [21,22] resolved structural characteristics at the level of 10 meV and determined that spiky structure exists only in approximant phases and not in QC. These calculations showed the non-existence spiky structure.

In this investigation we studied and report point contact tunneling experiments on  $\text{Tb}_9\text{Mg}_{35}\text{Zn}_{56}$  QC with high quasicrystalline structural order and high purity with second phases estimated below 2–5% level [2]. Differential conductance as a function of bias voltage shows the existence of a pseudogap. This characteristic depends where the contact spots are placed on the QC surface, in addition, the number of features observed increases as the  $n$ -fold surface increases. The results indicate that this pseudogap could be also related to a Kondo behavior or to a spin-glass feature present in this QC. In the studies carried out on three-fold surfaces, the point contact tunneling spectra show fine structure inside the pseudogap at temperatures below the spin-glass freezing temperature.

## 2. Experimental details

The spectroscopic observations in the studied quasicrystals show different structural characteristics on different surfaces when measured on two, three, and fivefold different regions. The spectroscopic features measured several times on different spots were always similar, considering that the point contact could change a little of the initial position. Schematically the setup is shown in Fig. 1. The determined characteristics were obtained with junctions of areas with few  $\mu\text{m}^2$ . The junction size is an important parameter in tunneling studies. The data collected in this study were the characteristics of very small surfaces. As the junction area increases fine features could be smoothed and only an average will be observed and the structure will be only the pseudogap feature.

Tunneling spectroscopy is one of the most sensitive probes to study the density of electronic states. It gives high spectroscopic resolution limited by temperature, thermal noise is the limiting factor. The thermal energy at 1 K is 86  $\mu\text{eV}$ . Therefore, with conventional modulation techniques, the energy resolution will be of this order of magnitude.

In point contact junctions, the relevant information will be related to scattering and dispersion of the elementary interactions in DOS and also on the features of the relevant spot on the surface. The  $dV/dI$ - $V$  data were measured at low temperatures with the normal tunneling electronic, consisting of lock-in amplifier, bridge, and modulation technique. The modulation consists of a sinusoidal signal at 1000 Hz with

amplitude below 50  $\mu\text{V}$ . Data was stored in a computer and inverted to obtain the differential conductance  $dI/dV$ - $V$ . The spectroscopic data was reproducible and observed many times in different parts of the QC studied. Tunneling spectroscopy is a difficult task and much precaution must be taken in order to probe that the measurement corresponds to tunneling or contacts currents [18]. One possible manner to probe the type of junction is by measuring and observing the superconducting energy gap when the sample or counter electrode is superconducting. In non-superconducting junctions other tests could be made, the so-called Rowell criteria. In this criteria, the differential resistance at zero bias as a function of temperature increases as the temperature decreases [23]. In a point contact junction the relevant characteristics will be related to pure Andreev reflections as the Blonder et al. model specifies [24]. In this work the point contact junctions were prepared as explained by Escudero et al. [18].

The QCs were fabricated and characterized by Fisher et al. [1,2]. The differential conductance versus energy (voltage)  $dI/dV$ - $V$  curves show structural features with different widths that change with temperature. The pseudogap feature was about a few mV, smaller than the size reported for Al-Pd-Mn, Al-Cu-Fe, and Al-Pd-Re specimens [17,18]. This small pseudogap could be related to the small resistances ratio between low and high temperatures as reported by Fisher et al. [1].

Spectroscopic measurements were performed on different sites of the QC surface, these sites are depicted in Fig. 1, furthermore, on regions of undetermined fold sites when the QC was broken. At low temperature the spectroscopic measurement reveals features, but not of the fine spiky nature. As the temperature is increased the structure and pseudogap become smoothed by thermal noise. Determination of the type of junctions, tunnel or metallic contact, depends of the thickness of the junction insulating barrier. Tunnel junctions formed with the native oxides grown on the QC surface sometimes were good enough to see tunneling characteristics. In many of the junctions studied the insulating layer was prepared by cleaning the specimen with diluted acid solution, washed with distilled water and finally exposed to the air. The exposed time was variable, from few minutes to hours. Moreover, we have to stress that the exposed time had only limited effect on the growing of the insulating layer, therefore the junction's differential resistances at zero bias  $(dV/dI)_{V=0}$  always presented distinct values. The  $(dV/dI)_{V=0-T}$  always increases from high to low temperature, in the range of 10 to 65  $\Omega$ . Junctions with small values behave as metallic point contact [23], with different temperature dependence of the differential resistance at zero bias; those were analyzed with the Blonder, Tinkham and Klapwijk model [24]. For this study we prepared more than 200 junctions (tunneling or metallic contacts), many presented reproducible features, those were used for this work, others were discarded. One important experimental condition, in order to have minimum averaging on the spectroscopic features, was to keep the junction area as small as possible.

To compare the spectroscopic characteristics of the QCs the  $dV/dI$ - $V$  curves of a polycrystalline Tb-Mg-Zn alloy were measured and observed. To obtain the Tb-Mg-Zn polycrystal a small part of the quasicrystal was wrapped with tantalum foil, placed into a quartz tube and encapsulated in argon atmosphere, heated at 700  $^\circ\text{C}$  and maintained at this temperature for 48 h. After this time the furnace was cooled slowly to room temperature. In this thermal process a small amount of Zn was lost. Additional measurements were performed in a Zn single crystal to compare with the QC.

The resulting information in this work was taken with junction formed with the QC specimen, the Tb-Mg-Zn polycrystal (named an approximant), and the Zn single crystal, as the first electrode of the junction. The second electrode was a thin Au-W wire with 5  $\mu\text{m}$  diameter, and cut in diagonal shape to have small dimension in the tip. The experimental setup for the junction, allows us to fabricate junctions with areas about 1  $\mu\text{m}^2$ . The setup allows to explore different regions on the QC surface by moving the second electrode to different spots.

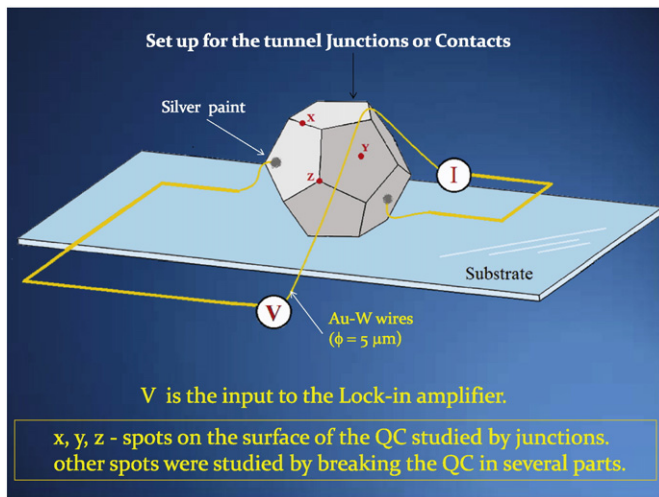


**Fig. 1.** Set-up for the point contact junctions in  $\text{Tb}_9\text{Mg}_{35}\text{Zn}_{56}$  an icosahedral quasicrystal studied with Au-W wires to form the junctions on different fold surface spots. Note that the quasicrystal is represented with the dodecahedral morphology.

### 3. Results and discussion

Spectroscopic data, obtained from a  $(\text{Tb}_9\text{Mg}_{35}\text{Zn}_{56})-(\text{Au}-\text{W})$  junction are shown in Fig. 2a and b, these curves were taken on a twofold surface. The curves shown in Fig. 2a are asymmetric, this characteristic is typical of tunneling currents [25]. In this figure the pseudogap feature is more pronounced when the temperature decreases. Note that at 15 K, the feature is small  $\pm 38$  mV and at 8 K the pseudogap is about  $\pm 55$  mV. Fig. 2b shows data of a contact on a twofold surface measured in different spot area of Fig. 2a. The pseudogap observed at 7 K is  $\sim 16$  mV, small than the observed in Fig. 2a. Moreover, two additional characteristics are seen, the differential resistance versus bias voltage in the range  $\pm 50$  mV is almost parabolic, and above those voltages is linear. The curves at 10 and 15 K do not show the pseudogap feature. The second characteristic is the symmetry of  $dV/dI-V$  curves. At this moment we do not have a simple explanation of this behavior, nevertheless taking into account that there are not theoretical models appropriate to interpret tunneling or contact measurements on QCs, the McMillan and Mochel [26], and Altshuler et al. [27] models give a reasonable fit to the experimental data. These models predict that DOS depresses near the Fermi energy as  $\sqrt{E}$ . In Fig. 2a and b the curves at low temperature between  $\pm 50$  mV show this energy behavior related to the formation of the pseudogap, and to localization, screening, and correlation effects different to as observed in conducting and crystalline alloys.

Figs. 3 and 4 show differential conductance  $dI/dV-V$ , on two spots of the threefold surface. These figures display curves measured at different temperatures where the temperature evolution of the pseudogap is observed. In Fig. 3 at 15 K the feature is only a minimum at the zero bias with features at high bias, at this temperature the pseudogap size is 19 mV. Decreasing the temperature,  $dI/dV-V$  shows fine structure in the interval  $\pm 35$  mV; the pseudogap is well defined at low temperature and shows asymmetric structure, a parabolic shape is well fitted from 15 to 6 K. Again this is a different behavior as seen in normal metals and may be related to the tendency to localization and increase of

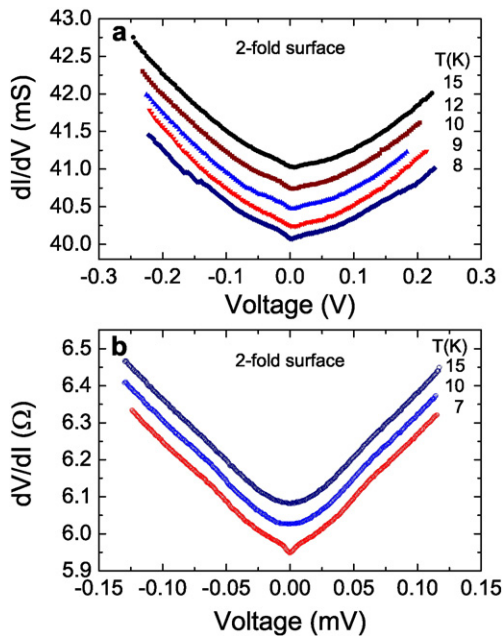


Fig. 2. (a) Differential conductance curves  $dI/dV$  versus voltage of  $(\text{Tb}_9\text{Mg}_{35}\text{Zn}_{56})-(\text{Au}-\text{W})$  tunnel junction measured from 15 to 8 K on twofold surface spot. At the Fermi level (zero bias) the small depression is the pseudogap and is about 38 mV size. At 8 K the pseudogap increases to about 55 mV. Note that the structure is asymmetric around zero bias. (b) Point contact differential resistance–bias voltage measured at 15, 10 and 7 K. The pseudogap on this twofold surface spot of the QC is only observed at low temperature. In addition, at 7 K the differential resistance shows a tiny structure about  $\pm 50$  mV, and the size of the pseudogap feature is only  $\sim 16$  mV.

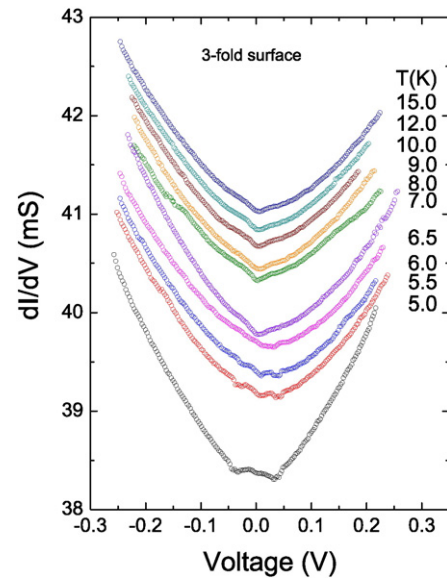


Fig. 3.  $dI/dV-V$  determined on a threefold surface spot of the QC. Note the structure in the pseudogap below 7 K. Above this temperature only a single feature was observed. At 15 K the pseudogap value is 19 mV. Observe that the total structure from  $\pm 200$  mV is highly asymmetric around Fermi level.

screening. Fig. 4a and b, shows data with similar spectroscopic features in Fig. 3. In Fig. 4b we present the same data of Fig. 4a, but amplified from  $\pm 100$  mV, note similar features as in other threefold surface. The tendency to smoothing the features is clear as the temperature is increased. Fine features can be distinguished from  $\pm 50$  mV, Fig. 4a shows data at  $\pm 300$  mV. Junction characteristics of Figs. 3 and 4 were made with Al and Au–W wires as second electrodes. Both  $dI/dV-V$  characteristics show similar behavior indicating that this is independent of the second electrode.

The  $dI/dV-V$  curves obtained from spots on threefold QC surface show features that resembled the electronic density of states determined by theoretical calculations [21,22] proposed in a three-dimensional Penrose tiling applied to  $\alpha$ -AlMn, Al–Pd–Mn QC and approximants. The main conclusion in these theoretical studies is related to the absence of spiky fine structure on DOS.

Data on fivefold spot were measured and plotted in Fig. 5 from 6 to 60 K. The characteristics can be seen in the interval  $\pm 300$  mV. A small

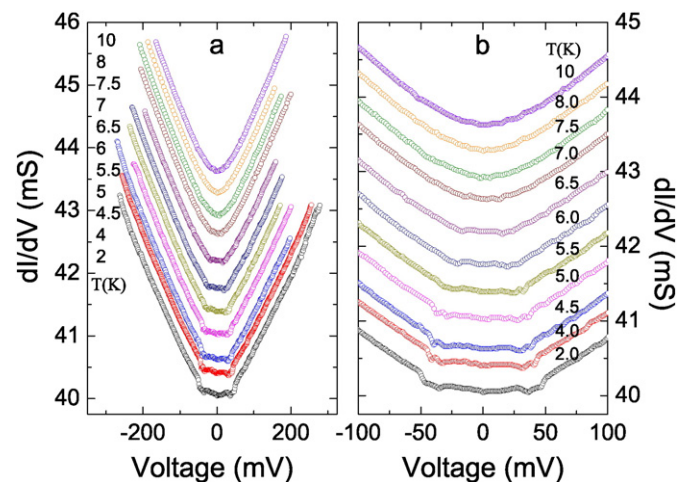
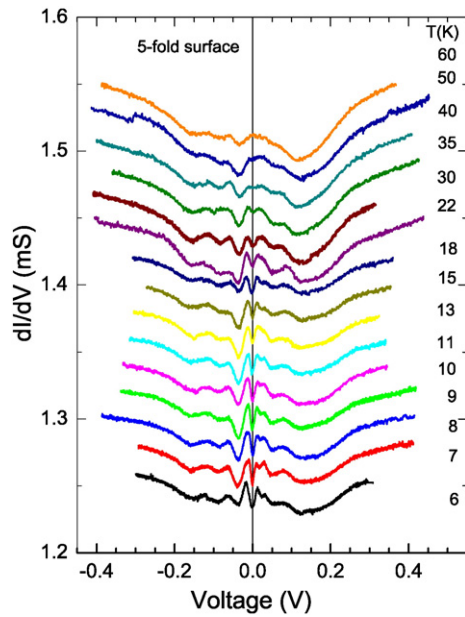


Fig. 4. Differential conductance data determined on a threefold spot. Panel a shows data measured between  $\pm 300$  mV. Note the parabolic shape at high temperature. Panel b is an amplification of panel a. Structure between  $\pm 50$  mV, at low temperature is reduced from 2 K up to 7 K.



**Fig. 5.**  $dI/dV-V$  data obtained on a fivefold surface. Structure is observed up to  $\pm 250$  mV. At Fermi level a pseudogap of  $\pm 20$  mV is observed, it decreases as the temperature increases. The pseudogap almost disappears above 30 K, and is absent at 60 K.

single pseudogap feature is at  $\pm 20$  mV, decreasing as the temperature is increased. At 35 K the pseudogap is only a very small minimum disappearing at 60 K. At this high temperature, still structure exists in the energy range  $\pm 200$  mV. The characteristics observed in these curves are quite similar to the  $dI/dV-V$  curves reported by Widmer et al. [9] and Mäder et al. [10], obtained with scanning tunneling microscopy in the spectroscopic mode. These measurements were performed on specific places on a small area of a fivefold surface of *i*-Al-Pd-Mn QC. Those authors associate the  $dI/dV-V$  curves to LDOS. If the curve data is obtained on large surfaces, i. e.,  $10 \times 10$  nm<sup>2</sup>, the resulting  $dI/dV$  is averaged and the spectra could be considered almost the total DOS [9]. It is noteworthy that similar spiky features were observed on the fivefold surface of different icosahedral QCs. These results indicate that the fine spiky structure could be related to the fivefold surface.

To confirm the existence of structure at different regions of the QC, it was broken to perform tunneling on different parts without knowledge of the fold region. The features on sites of the QC were observed showing distinct variants depending on the folding area, but similar to the already spots previously measured, so the spectral features change depending on the different surface fold measured. It is important to mention that these junctions gave similar information as already observed; less structural features on two and more on fivefold surface.

In the experimental work reported here, we never observed spiky fine structure as claimed in theoretical studies. We emphasize that the spectroscopic resolution in our junctions is at the order of 86  $\mu$ eV, when determined at low temperature with small modulation to detect the differential resistance. More important was the quality of the QCs used [1,2]. We think that this result is a clear indication that fine spiky structure indeed is nonexistent. Related to the spectroscopy studied on the pseudogap, this was seen in all different spots, but with small different size. We believe that this difference must be related to surface characteristics and different oxide thickness and imperfections. However, it is important to mention that different junctions evaluated on the same spots show similar value of the pseudogap, but different size. So, two conclusions can be obtained; the size of the pseudogap is very sensible to the surface examined and orientation.

In order to study the influence of magnetic effects on the QC we applied magnetic fields in parallel and perpendicular directions to the plane of the junction, the morphology of the QC (imperfections, small

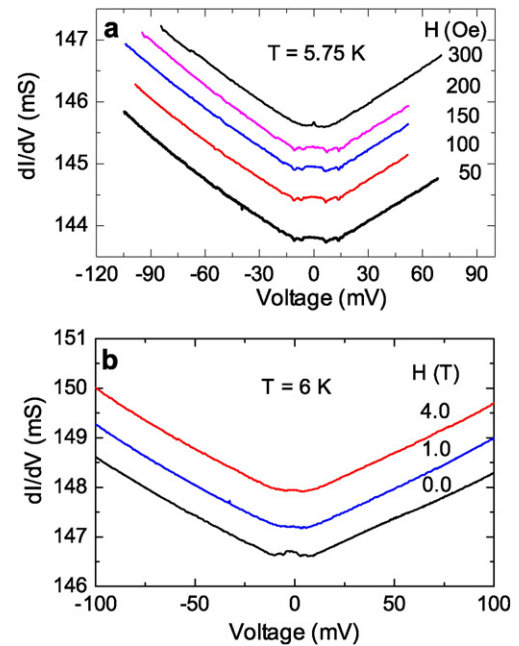


**Fig. 6.** Effect of the magnetic field on the differential conductance. Panel a) shows measurements performed at 5.75 K and low applied magnetic field. Panel b) shows the effect of 1 and 4 T over the tunneling characteristics measured at 6 K. In both cases the spectroscopic features are erased, but at 300 Oe appear only a small zero bias anomaly, meanwhile at higher field a flat region around zero bias remains.

size of the sample) was the impediment to precisely determine the QC directions on the applied magnetic field, nevertheless both measurements show similar characteristics and behavior. The structure around zero bias has a tendency to decrease and to be smoothed as the magnetic field is increased. Fig. 6a and b shows details of this behavior on a threefold surface with an applied field perpendicular to the point contact plane. Fig. 6a displays data at small magnetic fields from 50 to 300 Oe at  $T \sim 5.75$  K, close to the spin glass freezing temperature [28]. The pseudogap tends to decrease and shows only a small zero bias anomaly similar to Appelbaum type [29]. It is important to mention that according to Dolinšet and Jagličić [28] the spin glass behavior is not conventional, with differences as to a canonical spin glass. However, close to  $T \sim 6$  K and a high magnetic field, the structural features disappear, as shown in Fig. 6b, we do not have a plausible physical explanation for this behavior.

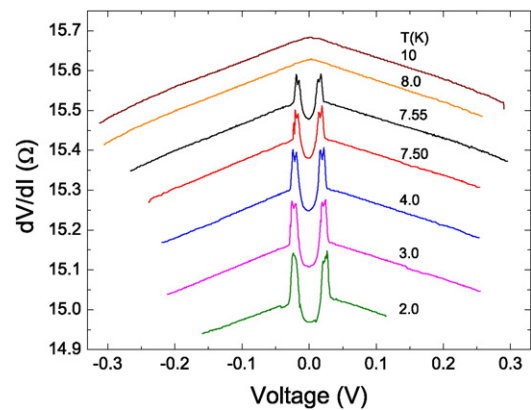


**Fig. 7.** Point contact differential resistance data of a spot on the surface of the QC. The feature may be related to a Kondo characteristic pseudogap, the size of this pseudogap is around  $\pm 40$  mV, probably related to the spin glass or antiferromagnetic coupling of Tb-Tb atoms. The temperature at which this feature appears is close to the spin glass freezing temperature.

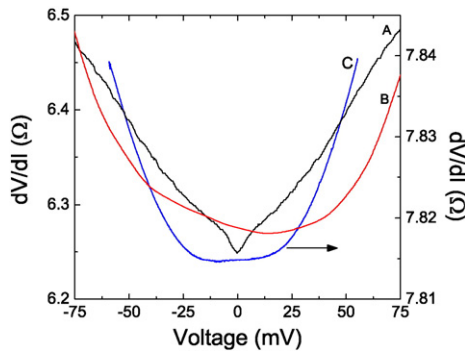


**Fig. 8.** Point contact differential resistance as a function of bias voltage of three different samples. Curve A is from a  $\text{Tb}_9\text{Mg}_{35}\text{Zn}_{56}$ -(Au-W) point contact measured at 7 K. Curve B is from a Tb-Mg-Zn polycrystal and gold wire, measured at 10 K. Curve C is from a Zn single crystal and gold wire, measured at 5 K. Note the depression around zero bias in the quasicrystal that we assigned as a pseudogap, it is not observed in curves B and C. The arrow indicates the vertical scale associated to curve C. Curve B was shifted up for an easy comparison with other curves.

An interesting piece of information is presented in Fig. 7. The curves were obtained on few spots of a new surface when the specimen was broken. The curves show a very well formed pseudogap, with symmetric structure at both sides of the Fermi energy. A possible explanation of this characteristic may be related to excess of Tb atoms in some non quasicrystalline regions of the sample. We think that these regions are so infrequent that they do not affect the magnetic behavior of the QC. The features are quite similar to the signature of Kondo effect, occurring by a possible hybridization gap [30] which arises by the influence of Tb  $f$  localized electrons and  $d$  conduction electrons. The size of this energy gap is  $\pm 40$  mV, it decreases as temperature increases disappearing at 8 K.

Lastly, we mention that the magnetic characteristics of  $\text{Tb}_9\text{Mg}_{35}\text{Zn}_{56}$  QC exhibit a Curie-Weiss type behavior with negative Weiss temperature, indicative of antiferromagnetic exchange interaction between the Tb atoms. Accordingly, this behavior has been related to spin glass characteristics presented below 5.8 K, the spin-glass freezing temperature [1,28].

Fig. 8 shows the curves of the already measured  $\text{Tb}_9\text{Mg}_{35}\text{Zn}_{56}$  QC, curve A, Tb-Mg-Zn polycrystal sample curve B, and Zn single crystal curve C. In this figure curve A is the same as of Fig. 2b, QC measured at 7 K. Curves B and C, were measured at 10 K and 5 K respectively. It is noteworthy that curve A clearly may be seen at zero bias diminishing of the differential resistance, interpreted as the pseudogap feature of the QC. Measurements of Tb-Mg-Zn polycrystal and Zn single crystal do not show the pseudogap feature, only show a flat region around zero bias. Those last experiments, shown in Fig. 8, were performed in order to demonstrate that the pseudogap observed is an electronic characteristic of  $\text{Tb}_9\text{Mg}_{35}\text{Zn}_{56}$  QC, this fact is in agreement with similar experiments reported for other QCs [17–20].

#### 4. Conclusions

We have demonstrated that a fine structure on the electronic density states indeed exists in  $\text{Tb}_9\text{Mg}_{35}\text{Zn}_{56}$  in spots of the QC studied. This experimental work shows different behavior to the theoretical

predictions of the existence of a spiky fine structure. The spectroscopic features determined at the different fold surfaces show that the number of structural features increases as the fold symmetry increases. Twofold spots present only a small pseudogap, moreover as the  $n$ -fold increases more features appear. The structure inside of the pseudogap is according to the theoretical studies by Zijlstra et al. [21,22]. In those theoretical studies they determined a pseudogap feature at the Fermi level using an ideal three dimensional Penrose tiling for the approximant and for a QC with compositions  $\alpha$ -AlMn and Al-Pd-Mn. Lastly, as a conclusion of our study we addressed that the study on QC needs more experimental and theoretical work in order to have better understanding, and perhaps these experimental results in Tb-Mg-Zn may be useful to improve this interesting field.

#### Acknowledgments

The single grain specimens were kindly provided by Prof. I. R. Fisher of Stanford University. We thank the interesting comments by E. Maciá, E. S. Zijlstra, E. Belin-Ferre, and D. Mayou. RE thanks to CONACYT and DGAPA-UNAM project IN106014.

#### References

- [1] I.R. Fisher, K.O. Cheon, A.F. Panchula, et al., *Phys. Rev. B* 59 (1999) 308.
- [2] I.R. Fisher, Z. Islam, A.F. Panchula, et al., *Philos. Mag. B* 77 (1998) 1601.
- [3] Y. Calvayrac, *J. Phys. IV* 6 (C2) (1996) 21.
- [4] M. Boudard, et al., *Philos. Mag. Lett.* 71 (1995) 11.
- [5] Z.M. Stadnik, D. Purdie, M. Garnier, et al., *Phys. Rev. Lett.* 77 (1996) 1777.
- [6] E. Belin-Ferré, C. Berger, M. Quinquandon, A. Sadoc (Eds.), *Quasicrystals: Current Topics*, World Scientific, Singapore, 2000.
- [7] E. Belin-Ferré, *J. Phys. Condens. Matter* 14 (2002) R789.
- [8] R. Rosenbaum, T. Murphy, B. Brandt, et al., *J. Phys. Condens. Matter* 16 (2004) 821; E. Maciá, *Phys. Rev. B* 61 (2000) 8771.
- [9] R. Widmer, P. Gröning, M. Feuerbacher, O. Gröning, *Phys. Rev. B* 79 (2009) 104202.
- [10] R. Mäder, R. Widmer, P. Gröning, W. Steurer, O. Gröning, *Phys. Rev. B* 87 (2013) 075425.
- [11] F.S. Pierce, S.J. Poon, B.D. Biggs, *Phys. Rev. Lett.* 70 (1993) 3919.
- [12] G. Kasner, H. Schwabe, H. Bottger, *Phys. Rev. B* 51 (1995) 10454 (and references therein).
- [13] D. Mayou, C. Berger, F. Cyrot-Lackmann, et al., *Phys. Rev. Lett.* 70 (1993) 3915.
- [14] Z.M. Stadnik, D. Purdie, Y. Baer, et al., *Phys. Rev. B* 64 (2001) 214202.
- [15] U. Mizutani, *J. Phys. Condens. Matter* 10 (1998) 4609; A.-P. Tsai, *J. Non-Cryst. Solids* 334&335 (2004) 317; U. Mizutani, T. Takeuchi, H. Sato, *J. Non-Cryst. Solids* 334&335 (2004) 331.
- [16] T. Fujiwara, T. Yokokawa, *Phys. Rev. Lett.* 66 (1991) 333; T. Fujiwara, S. Yamamoto, G. Trambly de Laissadière, *Phys. Rev. Lett.* 71 (1993) 4166.
- [17] D.N. Davidov, D. Mayou, C. Berger, et al., *Phys. Rev. Lett.* 77 (1996) 3173.
- [18] R. Escudero, J.C. Lasjaunias, Y. Calvayrac, M. Boudard, *J. Phys. Condens. Matter* 11 (1999) 383.
- [19] J. Dolinšek, M. Klanjšek, T. Apih, et al., *Phys. Rev. B* 62 (2000) 8862.
- [20] G.N. Banerjee, S. Banerjee, R. Goswami, *J. Non-Cryst. Solids* 334 (2004) 388.
- [21] E.S. Zijlstra, T. Janssen, *Phys. Rev. B* 61 (2000) 3377; E.S. Zijlstra, T. Janssen, *Europhys. Lett.* 52 (2000) 578.
- [22] E.S. Zijlstra, S.K. Bose, *Phys. Rev. B* 67 (2003) 224204.
- [23] B.J. Jönsson-Åkerman, R. Escudero, C. Leighton, et al., *Appl. Phys. Lett.* 77 (2000) 1870.
- [24] G.E. Blonder, M. Tinkham, T.M. Klapiwijk, *Phys. Rev. B* 25 (1982) 4515.
- [25] J.G. Simmons, *J. Appl. Phys.* 34 (1963) 1793.
- [26] W.L. McMillan, J. Mochel, *Phys. Rev. Lett.* 46 (1981) 556.
- [27] B.L. Altshuler, A.G. Aronov, *Zh. Eksp. Teor. Fiz.* 77 (1979) 2028.
- [28] J. Dolinšek, Z. Jagličič, *J. Alloys Compd.* 342 (2002) 377.
- [29] J.A. Appelbaum, L.Y.L. Shen, *Phys. Rev. B* 5 (1972) 544.
- [30] W.K. Park, P.H. Tobash, F. Ronning, E.D. Bauer, J.L. Sarrao, J.D. Thompson, L.H. Greene, *Phys. Rev. Lett.* 108 (2012) 246403.